Collision-Avoidance Characteristics of Grasping
Early Signs in Hand and Arm Kinematics

Janneke Lommertzen[1], Eliana Costa e Silva[2], Raymond H. Cuijpers[1], and Ruud G.J. Meulenbroek[1]

[1] Nijmegen Institute for Cognition and Information, Radboud University Nijmegen, Nijmegen, The Netherlands
[2] Department of Industrial Electronics, University of Minho, Guimarães, Portugal

Abstract. Grasping an object successfully implies avoiding colliding into it before the hand is closed around the object. The present study focuses on prehension kinematics that typically reflect collision-avoidance characteristics of grasping movements. Twelve participants repeatedly grasped vertically-oriented cylinders of various heights, starting from two starting positions and performing the task at two different speeds. Movements of trunk, arm and hand were recorded by means of a 3D motion-tracking system. The results show that cylinder-height moderated the approach phase as expected: small cylinders induced grasps from above whereas large cylinders elicited grasps from the side. The collision-avoidance constraint proved not only to be accommodated by aperture overshoots but its effects already showed up early on as differential adaptations of the distal upper limb parameters. We discuss some implications of the present analysis of grasping movements for designing anthropomorphic robots.

1 Introduction

Grasping objects is a task that people perform almost on a continuous basis. Such a seemingly simple task proves extremely complex when it comes to computationally describing the mechanisms that allow us to do so. For example, when developing anthropomorphic robots. Numerous studies have scrutinised the kinematics of this basic human motor skill, often quantifying typical kinematic landmarks such as peak velocities of the wrist trajectory that vary systematically as a function of (I) the distance between the starting location of the hand and the position of the to-be-grasped object, and (II) the evolution of the grip aperture, of which the size and timing vary systematically as a function of the size of the to-be-grasped object (Jeannerod 1981; Jeannerod 1984; Paulignan, Frak, Toni and Jeannerod 1997; Smeets and Brenner 1999; Meulenbroek et al. 2001; Smeets and Brenner 2001; Cuijpers, Smeets and Brenner 2004).

First we will give some background on research that focusses on collision avoidance behaviour in human prehension. Next, we describe collision avoidance techniques that are used in robotic manipulators including the **ARoS**

G. Pezzulo et al. (Eds.): ABiALS 2008, LNAI 5499, pp. 188–208, 2009.

(**A**nthropomorphic **Ro**botic **S**ystem), which is an anthropomorphic robotic system that was built on the Mobile and Anthropomorphic Robotics Laboratory group at University of Minho, Portugal (ARoS, Silva, Bicho, Erlhagen 2008). We will conclude our paper with a discussion of the implications of our experimental results for robotics, we show that our anthropomorphic robot (ARoS) is capable of reproducing human movement characteristics, thus facilitating interactions with humans, and we discuss some implications.

1.1 Obstacle Avoidance in Humans

Only few prehension studies take into account the ways in which grasping movements are tuned to avoid collisions with the target object or any intermediate object (see e.g. Vaughan, Rosenbaum et al. 2001, Butz, Herbort and Hoffmann 2007). The present study was conducted to fill this gap. Additionally, the collision-avoidance component of grasping forms an essential ingredient of the posture-based motion planning theory developed by Rosenbaum, Meulenbroek, Vaughan and Jansen (2001). This theory states that the aperture overshoots that are commonly observed when the hand shapes around to-be-grasped objects, or any other biphasic component of the movement pattern, are due to the collision-avoidance constraint inherent in grasping. This claim also prompted the present study.

It is still not fully understood how the human prehension system copes with collision avoidance. Some studies focussed on reach-to-grasp movements in the presence of distractor objects that may have acted as obstacles (Meegan and Tipper 1998; Kritikos, Bennett, Dunai and Castiello 2000). In these studies it was observed that the hand trajectory veered away from intermediate distractors. This tendency was regarded as an interference effect related to the inhibition of a planned movement towards the distractor. Humans smoothly adjust movements of their effector system to circumvent obstacles by planning a movement through a 'via point'(Edelman and Flash, 1987), or 'via posture' (e.g. Rosenbaum et al., 2001). Meulenbroek et al. (2001), emphasised, that in order to avoid collisions with intermediate objects while grasping a target object, moving around the obstacle requires a biphasic component that, when superimposed on the default movement plan that will bring the hand to the target in the absence of the obstacle, ensures that the obstacle is avoided with an acceptable spatial tolerance zone (see also: Vaughan, Rosenbaum et al. 2001). It should be noted that these models ignore the fact that an end posture depends both on start point and trajectory, a recent paper by Butz et al. (2007), describes a model (SURE_REACH), which adds a neural-based, unsupervised learning architecture that grounds distance measures in experienced sensorimotor contingencies. In this model, an obstacle representation can inhibit parts of the hand space, causing the arm to generate alternative movement trajectories when the inhibition is propagated through to posture space.

In the present study, we focus on how grasping movements of which the collision-avoidance characteristics were varied, are executed. To manipulate the degree with which target objects itself acted as obstacles, we chose two starting

positions at equal distances from the target location (see Figure 1). One from which a straight hand movement would suffice for a safe and successful grasp, and one from which additional arm-configuration adjustments were needed in order to prevent a collision of the hand with the target. In line with Meulenbroek et al. (2001), we expected movements with the right hand, starting to the right from the target (S2) to elicit a smaller effect of the collision avoidance constraint on the grasp (i.e. less or no additional arm-configuration adjustments) than movements starting from the left of the body midline (S1).

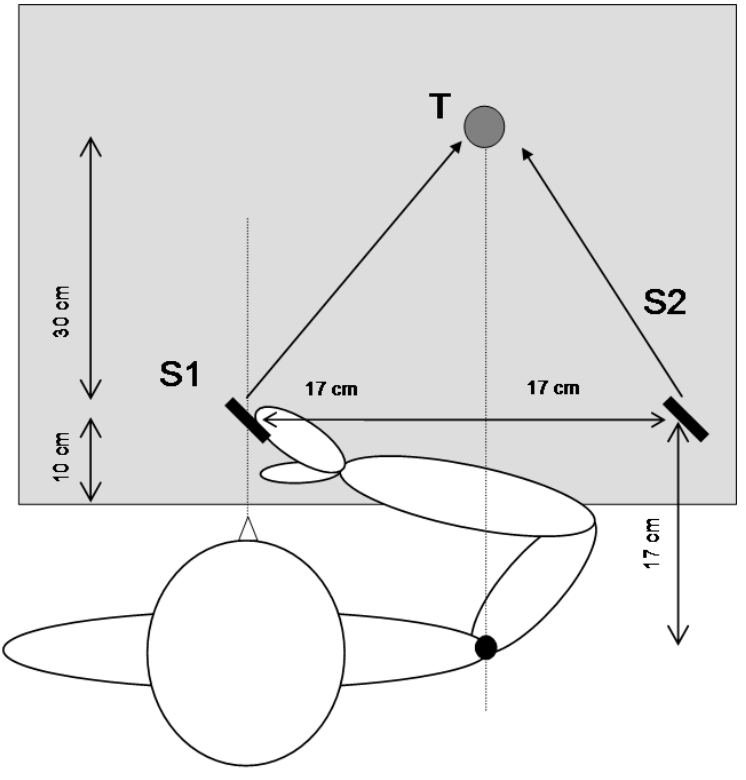

Fig. 1. Top view of experimental setup. 'S1' and 'S2' indicate the starting positions, and 'T' the target location.

Another way we manipulated the risk of collision was to vary the height of the target cylinders between 1 to 15 cm. Conceivably, collision with the shallowest cylinders is easily avoided by moving the fingers over the target cylinder before grasping it, whereas such a grasping strategy would probably be inefficient for the tallest cylinders. For the tallest cylinders, a lateral approach of the hand was expected since lifting the arm upwards against gravity to manoeuvre the hand above the cylinder top, was considered energetically suboptimal.

1.2 Collision Avoidance in Robotics

The simplest way to model a grasping movement would be to compute the required hand trajectory or joint rotations necessary to move from the starting posture to the final posture. This can result in successful grasps in some cases but will often result in a movement during which part of the effector system will collide, or even virtually move through the target object. Knowledge about how humans adjust their movements when avoiding collisions with obstacles is necessary if one attempts to develop robots that can safely interact with humans (Erlhagen et al. 2006). The latter challenge for roboticists formed the applied context that inspired the present study.

Typically, the human arm is modelled as a rigid stick-figure of seven degrees of freedom (DoF): three DoFs in the shoulder, one in the elbow, and three in the wrist. Only six DoF are needed to describe the position and orientation of the hand in Cartesian space (x, y, z, and Rx, Ry, Rz). Thus one degree of freedom remains that enables multiple joint configurations to result in the same hand position and orientation. This allows us to smoothly avoid obstacles or to choose the most efficient movement path out of numerous possibilities. It should be noted that the hand itself also has many degrees of freedom and that stretching and flexing of the fingers also plays a role in obstacle avoidance behaviour. But for this paper we focus on the upper limb with only two fingers as 'gripper'. We use an anthropomorphic robotics system (ARoS, Silva et al., in press), with a similar configuration for simulating reaching and grasping cylindrical objects in 3D space, as described below.

1.3 Antropomorphic Robotic System (ARoS)

The ARoS model is based on observations from experiments studying the human upper limb: (I) movement planning is done in joint-space (Osheron, Kosslyn and Hollerbach 1990; Rosenbaum 1990), (II) joints move in synchrony (Klein Breteler and Meulenbroek 2006); (III) planning of a reaching and grasping movement in joint space is divided into two sub-problems: (a) end posture selection and (b) trajectory selection (Meulenbroek, et al. 2001; Rosenbaum et al. 2001; Elsinger and Rosenbaum 2003) [1], (IV) end posture is computed prior to trajectory (Gréa, Desmurget and Prablanc 2000; Elsinger and Rosenbaum 2003), (V) end posture varies as a function of initial posture (Soechting, Buneo, Herrmann and Flanders 1995; Fischer, Rosenbaum and Vaughan 1997), and (VI) obstacle avoidance is incorporated by a mechanism that superposes two movements: a direct movement from the initial to the end posture and a via movement from the initial posture to the via posture and back (Rosenbaum, Meulenbroek et al. 1999; Meulenbroek, Rosenbaum et al. 2001; Vaughan, Rosenbaum and Meulenbroek 2006). First, the most adequate end posture is determined by choosing the posture that can be obtained such that the object is successfully grasped without collisions with any

[1] By posture we mean the set of joint angles of the arm and hand. Posture is represented using the well known, and widely used in robotics, Denavit-Hartenberg (proximal) convention (Craig 1998).

obstacle or the target itself at the moment of grasp, with a minimum displacement of the joints from begin to the end of the movement. Different joints may have different expense factors that contribute differently to the selection of end posture and trajectory.

Next, the trajectory of the joints is computed. We applied the minimum jerk principle to the joints of the arm and hand, such that the default movement of the joints follows a bell-shaped unimodal velocity profile, resulting in a smooth straight-line movement in joint space.

If this direct movement does not lead to collisions with obstacles, the movement is performed, otherwise a 'via movement' is added to the default movement by finding a detour through joint space that is collision-free. This via movement is a back-and-forth movement from the initial posture to a promising via posture and back again to the initial posture. The 'via movement' is superimposed on the direct movement and both are performed simultaneously.

2 Method

2.1 Participants

Twelve participants, (4 male, 8 female), ranging in age between 20 and 34 years (mean = 28 years) were included in the analyses of this study. All participants participated for course credit or remuneration after giving their informed consent.

2.2 Procedure

Participants sat comfortably at a table on a height adjustable chair and they were asked to make prehension movements from one of two starting positions and to grasp a target cylinder that could vary in height. The table was mounted with a board, on which two small strips of sandpaper were stuck to indicate the starting positions, and a circular hole was sawn out to indicate the target position (see Figure 1).

Participants started each trial with the index finger of their right hand aligned with one of the two strips of sandpaper that indicated the start locations. Upon hearing the auditory 'go'-signal, participants moved their right hand from one of two start locations to the target cylinder, grasped the target between thumb and index finger, and, as soon as a second auditory cue sounded, lifted the target briefly put it back on the table, and returned their hand to the start location (see Figure 2). During the response sequence we recorded the 3D movements of the index finger, thumb, hand, wrist, upper arm, and trunk, and we evaluated various kinematic variables normalised in time.

Movements were recorded by means of two Optotrak camera units (Optotrak 3020, Northern Digital). Recordings were made for 5 s with a sampling frequency of 100 Hz, of the trunk, upper arm, wrist, hand, and thumb and index finger. The thumb and index finger trajectories were recorded using single markers that were attached to the tips of the nails of these digits. All other movements were

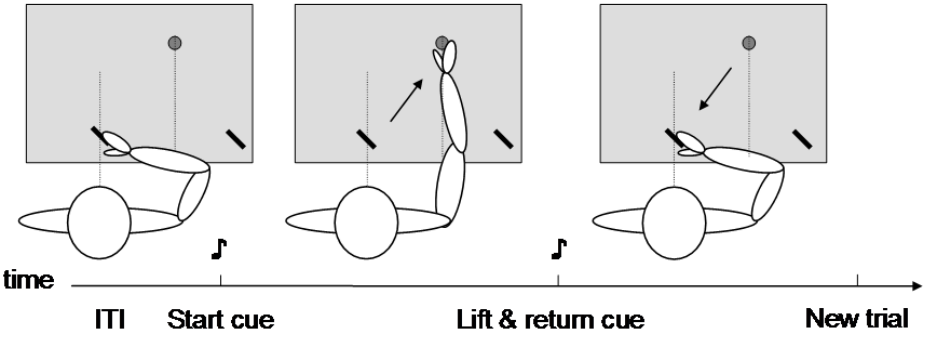

Fig. 2. Timing of trial events. A top-view example of a trial starting from S1 (left panel). As soon as the start cue sounds, the participant reaches out and grasps the target cylinder (central panel). Then the participant waits until the second auditory cue is sounded, lifts the cylinder, puts it back on the table, and returns to the starting position to prepare for the next trial (right panel). (ITI = Inter-Trial Interval).

recorded by means of rigid bodies (RB). RBs consist of minimally three IRED markers (the wrist and hand RB had four IREDs) at fixed positions relative to each other. This enables recording of not only the spatial location, but also the spatial orientation (Euclidean rotations around the x, y, and z- axes, see: Bouwhuisen, Meulenbroek et al. 2002). A specific calibration procedure allowed us to look at the relative orientations of the body segments making up the kinematic chain of the arm, hand and fingers. The orientation of the upper arm RB was recorded relative to the orientation of the trunk RB, the orientation of the wrist RB was recorded relative to the upper arm RB, and the orientaton of the hand RB relative to the wrist RB. This way, the upper arm RB rotations give an estimate of the rotations in the shoulder joint around three axes in Cartesian space (Bouwhuisen, Meulenbroek and Thomassen 2002). The displacements of the individual markers and the trunk RB were recorded relative to an external reference frame with the x-axis aligned with the horizontal, frontoparallel line, the y-axis with the horizontal, midsaggital line, and the z-axis with the vertical.

In order to induce obstacle avoidance behaviour during this task, we manipulated two factors, the Starting Position and the Target Height. We used eight different target cylinders with a diameter of 4.5 cm that were 1, 3, 5, 7, 9, 11, 13 and 15 cm tall. The central Starting Position (S1) was about 17 cm directly in front of the body midline on the tabletop and the lateral starting position was about 17 cm laterally in front of the shoulder. The target location was at about 47 cm distance from the trunk and at equal distance from the two start locations (see Figure 1). In order to induce different movement speeds, we also manipulated the response window, i.e. the interval in which participants had to perform their grasping movements. We did this because we assumed that extra time stress would force/stimulate the participants to use the most efficient movement plans (Rosenbaum et al. 2001).

2.3 Design

In every alternating block the Starting Positions changed, and eight Cylinder Heights were quasi-randomly repeated twice. Every participant performed 196 trials, run in twelve blocks of 16. The response window, i.e. the time interval between the starting cue and the lifting cue changed after half of the trials. Half the participants started with the fast condition (i.e. 1.5 s prehension interval), and the other half of the participants started with the slow condition (2 s prehension interval).

2.4 Analyses

Position and rotation data were linearly interpolated in case of missing data (which occurred infrequently and never more than 10 successive samples), and filtered by means of a Butterworth filter with a cut-off frequency of 12 Hz. Computed velocities were filtered with a cut-off frequency of 8 Hz. Trials with too many missing samples were excluded from further analyses, in total (2.7%) of all trials.

We only analysed the first part of the response sequences, i.e. the movements from start to the end of the grasp. Begin and end of this movement phase were deduced from the tangential velocity of the grip, defined as the magnitude of the first derivative of the mean position of thumb and index finger (as measured by the respective IREDs). The start of the movement was defined as the last local minimum in the tangential grip speed profile before it exceeded the threshold of 5% of the maximum tangential grip speed, and the end of the movement was defined as the first local minimum in the speed profile after it dropped below this threshold again (after the maximum velocity was reached). After the beginning and end of the prehension phase were determined, all displacements, rotations, and derived variables were normalised to time and resampled to 50 samples.

Because we were interested in different grasping strategies, we looked at the ways participants approached the cylinders, i.e. whether they approached the cylinder with their hand from the side, or whether they moved their hand over the top of the cylinder before completing their grasping. To this aim, we analysed the locations of the fingertips relative to the centre of the hand -as defined by the rigid body of IREDs attached to it- in the horizontal plane. The cylinder is defined as a circle with a radius of 2.25 cm centered at the origin. The finger trajectories were translated such that the final locations of thumb and index finger were positioned on the cylinder. We also determined the amount with which the line connecting the location of the index finger and the centre of the hand swept across the circle that defined the cylinder's top. Trials in which this occurred, were labelled as Overlap (OL) (see Figure 3A for an example) and all other trials, in which the cylinder was approached and grasped from the side, were labeled as No Overlap (NoOL).

The most important variable we manipulated to induce obstacle avoidance behaviour was the cylinder height. Because we expected the grip height to depend on the target height, we first looked at the grip height in time. Grip height is the mean z-coordinate of thumb and index markers, and therefore a good indicator of the behaviour of the most distal part of the effector system.

Because we aimed at inducing obstacle avoidance behaviour, which we also expected to be reflected in biphasic velocity profiles, we also studied the tangential velocity profiles of the grip (i.e. the average position of the thumb and index markers).

Since participants were instructed to start their responses with their hand flat on the table top, it is also interesting to study the change in hand orientation in time. To this aim, we computed the hand plane angle (HPA). HPA was defined as the angle between the horizontal plane and the plane that is defined by the marker of the hand RB closest to the MCP-II joint, the index marker, and the thumb marker. A horizontal position (palm down) is defined as 0 deg, and a vertical orientation with the thumb down is defined to be 90 deg. We expected the HPA to start near horizontal, to become more vertical during the prehension phase, and rotate back to a more horizontal posture towards the end of the grasp.

Because we expected differences in obstacle avoidance to be reflected in the relation between proximal and distal parts of the effector system, we contrasted the HPA with the arm plane angle, which is defined as the angle between the horizontal plane and the plane that is spanned by the vectors denoting the upper arm RB and the wrist RB.

To compare the proximal and distal involvement (i.e. the shoulder and wrist) in the grasping movements at joint level, we computed the net shoulder (Rs) and wrist (Rw) rotations as the square root of the sum of the squared rotations around the x, y, and z-axes of the upper arm RB relative to the trunk RB (Rs), and of the hand RB, relative to the wrist RB (Rw), as described in Eq. 1.

$$Rw, s = \sqrt{Rx^2 + Ry^2 + Rz^2} \tag{1}$$

where for the shoulder rotation (Rs), Rx, Ry, and Rz are the rotation angles of the upper arm RB relative to the trunk RB, and for the wrist rotation (Rw), Rx, Ry, and Rz are the rotation angles of the hand RB relative to the wrist RB. These rotation measures are independent of rotation direction, and give an estimate of the degree of rotation in the specific joint.

After deriving all these variables, every time series of these variables was normalised in time to 50 samples. This way we were able to compare trials with different durations.

3 Results

First we established that our experimental manipulations were effective in causing different types of obstacle avoidance behaviour, as reflected by different ways

Table 1. Incidence (number of trials) of the two distinguished Grip Types (NoOL = No Overlap grip; OL = Overlap grip) as a function of Starting Position (Start=1 and Start=2) and Cylinder Height (in cm)

	Start = 1	Start = 1	Start = 2	Start = 2
Cylinder Height (cm)	No OL	OL	NoOL	OL
1	49	94	117	26
3	87	56	131	13
5	116	28	133	10
7	123	20	140	4
9	129	12	142	2
11	134	8	141	3
13	137	5	141	2
15	138	4	139	5
Grand Total	913	227	1084	65

to approach and grasp the target cylinder. Figure 3 shows examples of grasping responses to the shallowest and highest cylinders from both starting locations. Participants moved their hand over the top of the target cylinder in some trials, and approached the cylinders sideways in other trials. As mentioned before, we labeled the trials in which participants moved their index finger over the cylinder as "Overlap trials" (OL) and all other trials as "No Overlap trials" (NoOL). Figure 4 and Table 1 show the overall number of OL trials per starting position plotted against cylinder height. Note that the shallowest cylinders are most often grasped with an overlap grip, and that this occurs most often in responses starting from S1, as we expected.

3.1 Grip Height

After having established that varying start location and cylinder height yielded different grasp types, we focused on how our main variables of interest varied as function of cylinder height and start location. As expected, the grip height increases and decreases in time, and differentiates between different cylinder heights (see Figure 5). The moment at which the grip height starts to differentiate between different cylinder heights was captured by analysing the time-normalised standard deviations (SD) across cylinder heights (see Figure 5B). 'Kick-in' was defined as the moment at which the SD reached the threshold of 1% of the range of grip heights. This analysis clearly shows that the effect kicked in early on in the movements, in particular already at 10% of the movement time.

3.2 Arm-Plane Angle and Hand-Plane Angle

Now we know that the kinematic variable grip height, that characterises the most distal part of the upper limb is affected by the target height, it is interesting to look at two other variables that -together- incorporate the whole movement of the upper limb. The Arm Plane Angle (APA) and Hand Plane Angle (HPA) are

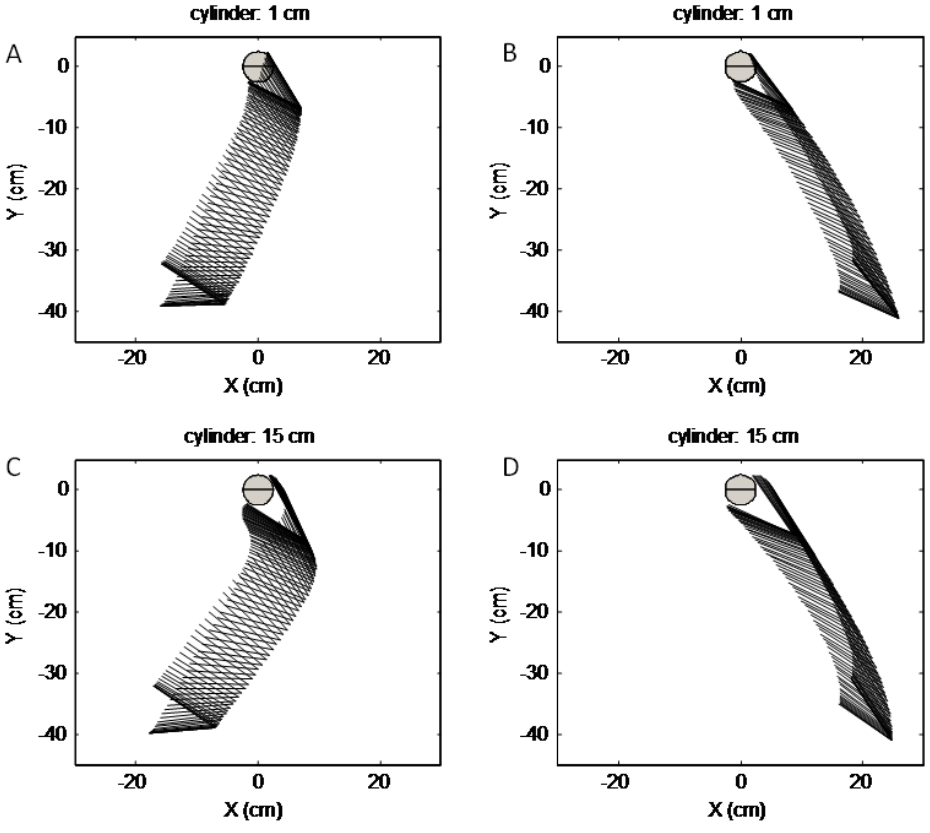

Fig. 3. Top view of the position changes of the hand in the horizontal plane during individual grasps. The bottom black line of the V-shapes connects the centre of the hand RB with the IRED on the tip of the thumb; the top black line of the V-shapes connects the centre of the hand RB with the IRED on the tip of the index finger. (A) from S1 to the shallowest cylinder with an Overlap grip, (B) from S2 to the shallowest cylinder with a No Overlap grip, (C) from S1 to the tallest cylinder with a No Overlap grip, and (D) from S2 to the tallest cylinder with a No Overlap grip. See also Figure 1.

shown as a function of normalised time in Figure 6, revealing that HPA varies with cylinder height, whereas APA shows a very stable pattern across cylinders (see Figure 6A, C). The final APA and HPA are shown in Figure 6C and D.

To find the moment at which the effect of cylinder height on the HPA kicked in, we used the same method as earlier described for the grip height:

The moment at which the standard deviations of APA and HPA started to differentiate was defined as the moment the difference between the SDs of APA and HPA reached the threshold of 1% of the mean range of SD(HPA) and SD(APA). This occurred at 12% of movement time for S1 and at 20% of movement time for S2 (see Figure 6B).

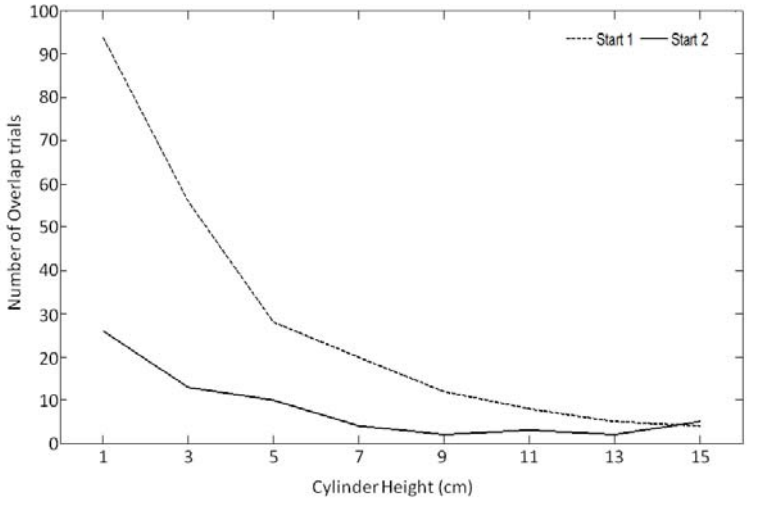

Fig. 4. Number of trials with an overlap grip counted across all participants, for every cylinder height. The dashed line represents Start 1 and the solid line represents Start 2.

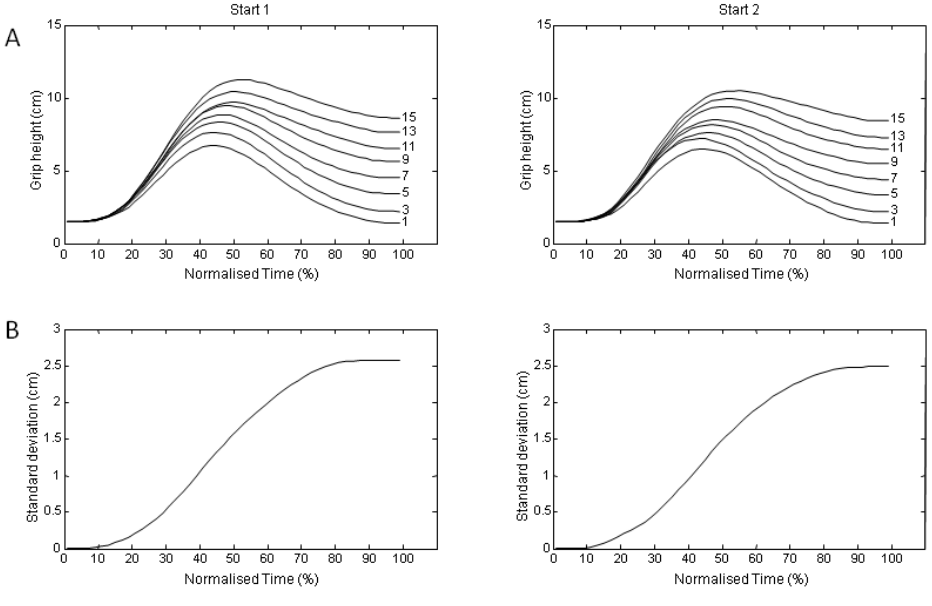

Fig. 5. (A) Time-normalised Grip Height changes for Start 1 and Start 2, averaged across participants (N=12). Different lines represent different cylinder heights, as indicated by the numbers at the righthand-side of the curves. (B) Standard deviations across cylinder heights as a function of time for Start 1 (bottom left) and Start 2 (bottom right).

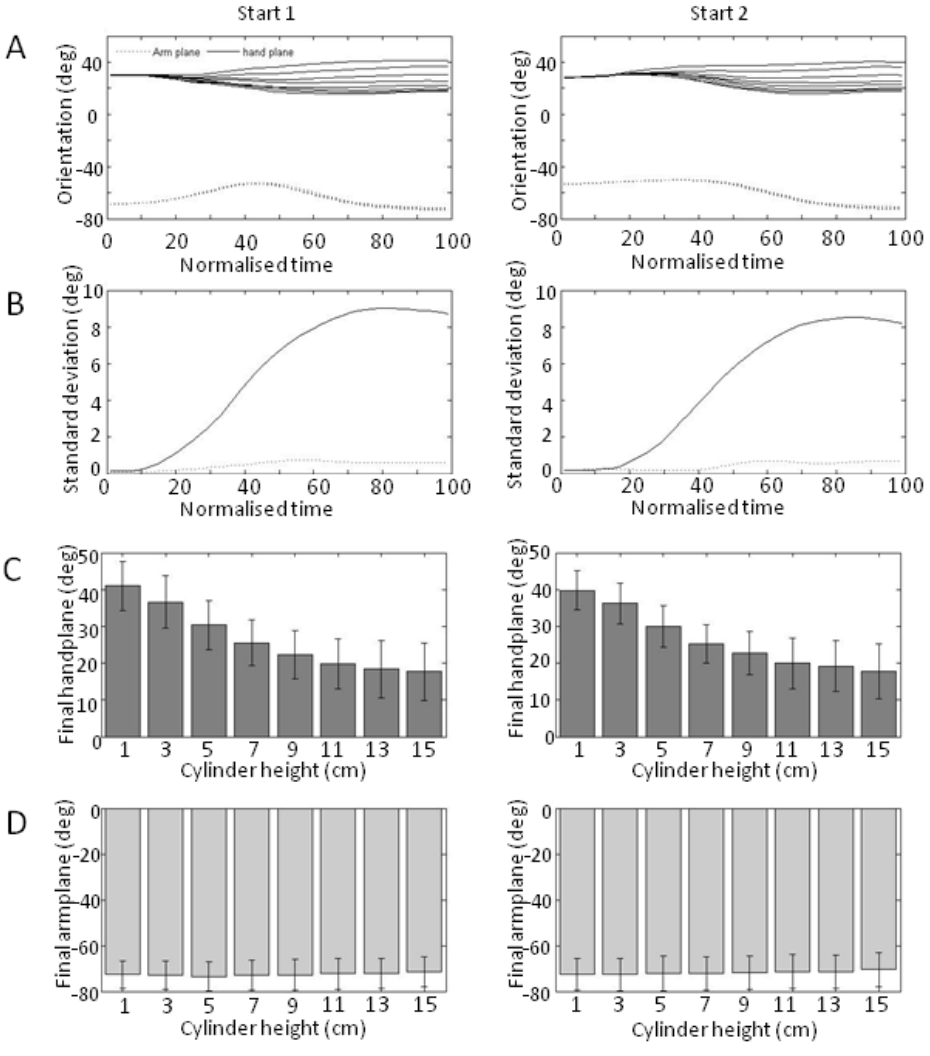

Fig. 6. (A) Arm-plane (solid lines) and hand-plane (dashed lines) angles (deg) in time for Start 1 and Start 2. Different lines represent different cylinder heights. (B) Standard deviation across cylinder heights in time for Start 1 and 2. (C) Final hand plane per cylinder height, averaged across cylinders for Start 1 and Start 2, (D) Final arm plane per cylinder height, averaged across cylinders for Start 1 and Start 2.

3.3 Wrist Rotation and Shoulder Rotation

A similar approach can also be applied to a comparison of the net shoulder and wrist rotations (Rs and Rw). Figure 7A shows that wrist-rotation patterns overlap in some cases, but still differentiate more between cylinder heights than the shoulder rotation patterns do (see also the final Rw and Rs, as plotted in Figure 7C,D).

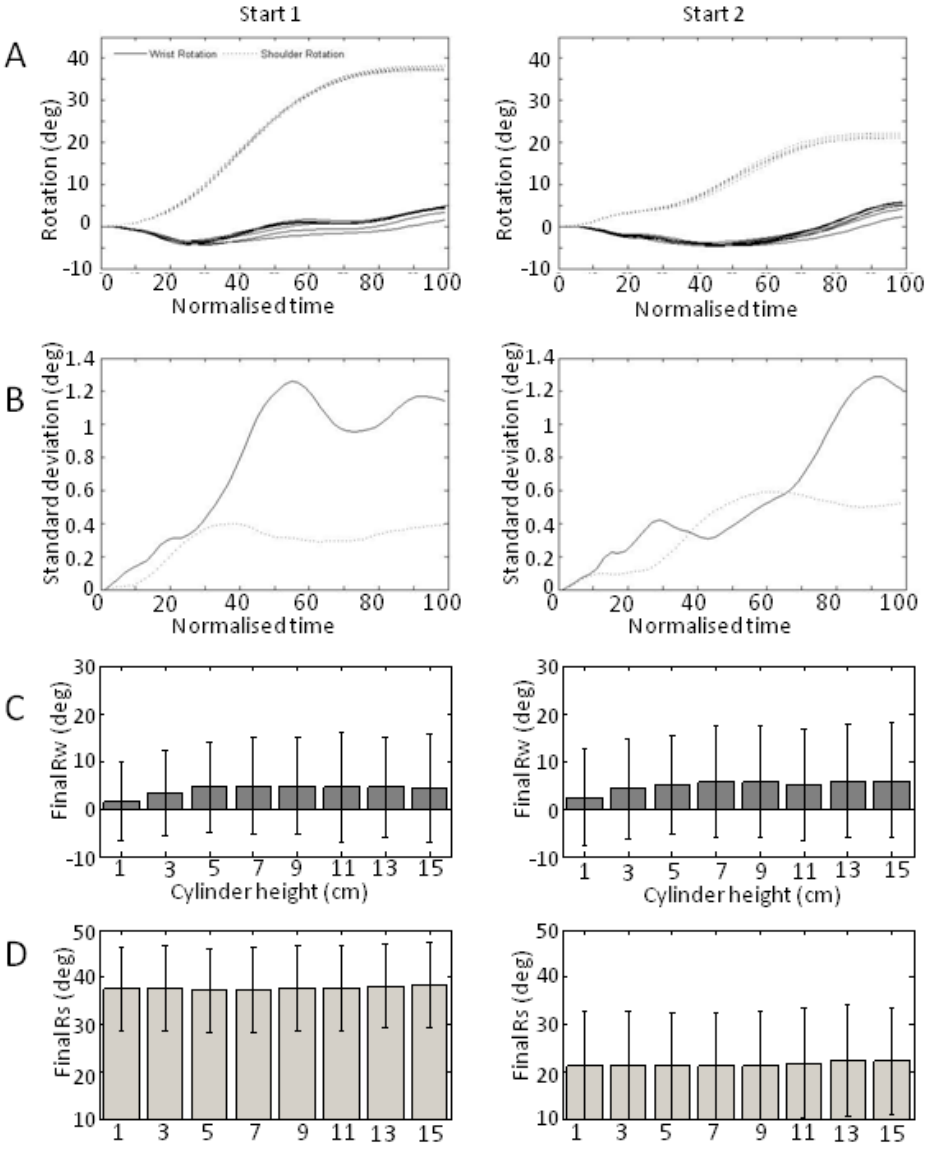

Fig. 7. Wrist rotation (solid lines) and shoulder rotation (dashed lines) in time for Start 1 and Start 2. Different lines represent different cylinder heights. (B) Standard deviation for wrist- (solid line) and shoulder rotation (dashed line) across cylinder heights in time for Start 1 and 2. (C) Final wrist rotation per cylinder height, averaged across cylinders for Start 1 and Start 2, (D) Final shoulder rotation per cylinder height, averaged across cylinders for Start 1 and Start 2.

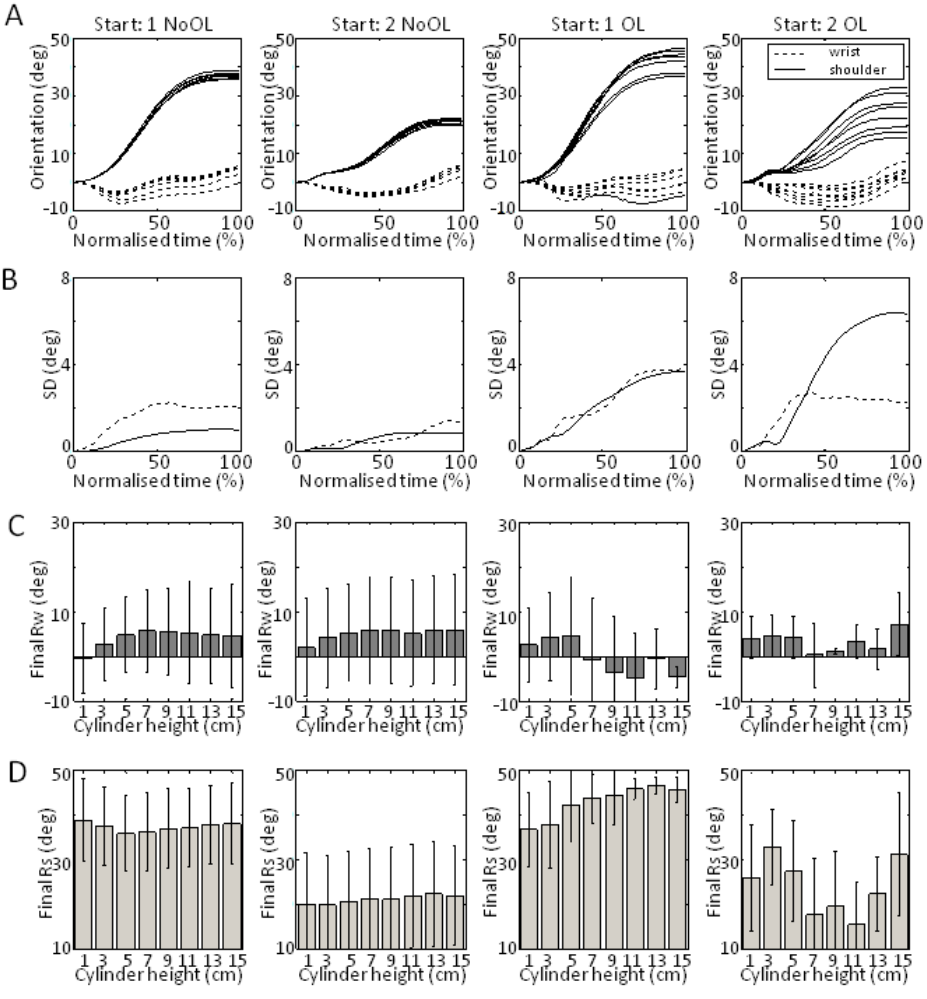

Fig. 8. Wrist rotation and shoulder rotation. Columns represent the two starting positions and grasp types (Overlap and No Overlap) (A) Wrist rotation (solid lines) and Shoulder rotation (dashed lines) in time. Different lines represent different cylinder heights. (B) Standard deviation for wrist- (solid line) and shoulder rotation (dashed line) across cylinder heights in time. (C) Mean final wrist rotation per cylinder height (D) Mean final shoulder rotation per cylinder height.

SDs computed across cylinder heights, are larger for the wrist rotation than for the shoulder rotation (see Figure 7B). Furthermore, the SD patterns seem to differ for the two start locations, suggesting that the effects of the Cylinder Height kick in later during the response in responses starting from S2 than from S1. The difference between Rw and Rs is also evident in Figures 7C,D: the final wrist rotation angle (Rw) differs slightly between the shortest cylinders, whereas final shoulder rotation angle (Rs) is stable across cylinder height.

The difference we observed between the rotation patterns for the two start locations might be related to the effects of Overlap and No Overlap grasps. To evaluate this aspect, we also compared the development of these variables between the two grip types (See Figure 8). Both the wrist and shoulder rotation were most strongly affected by the cylinder height in the OL trials, presumably because participants grasped the cylinders near the top. The development of SDs across cylinder heights, as shown in Figure 8B showed steeper SD curves for the OL trials, and this was most pronounced in the wrist rotation. It should be noted that OL and NoOL trials were not equally distributed across participants and conditions (see Table 1), therefore it is hard to statistically test these data patterns.

3.4 Speed Instructions

Movement time was compared between the two Speed Instruction conditions and the two Starting Positions by means of a 2 x 2 repeated measures ANOVA. The participants followed the speed instructions; movements in the high-speed instruction condition took less time than in the low-speed condition (914 ms and 967 ms, respectively; $F(1, 13) = 6.228; p < .05$). Movements starting from S2 lasted longer than from S1 (910 and 972 ms, respectively; $F(1, 13) = 45.542; p < .001$). There was no interaction between Speed Instruction and Starting Position.

4 Discussion

One of the main purposes of our experimental study was to gain more insights in the ways upper-limb movements are altered in order to prevent collisions with a target to-be-grasped. The paradigm we used showed that participants roughly used two collision-avoidance strategies: circumnavigating the cylinder and approaching from the side (NoOL grip), or approaching it from above (OL grip). As expected, the OL grip types occurred more frequently in the trials starting from S1 than S2, because the shortest trajectory from start to target would collide with the cylinder starting from S1 but not from S2. OL grip types occurred also more frequently when shallow cylinders had to be grasped, because lifting the hand over the cylinder requires less effort for shallow cylinders than taller ones.

We analysed the time-normalised grip height, hand-plane angle (HPA), arm-plane angle (APA), wrist- and shoulder rotations (Rw and Rs) for the two starting positions and all cylinder heights. APA and Rs did not show any target height-dependent patterns. There seems to be some differentiation in Rw for the shortest cylinders, but the strongest effects of target height were reflected in the time-normalised Grip height and HPA -patterns. These height-effects were present immediately at the start of the response for the HPA, and at 10% of movement time for the grip height. Showing that the more distal parts of the effector system are more sensitive to slight alterations in task requirements than proximal parts.

Because Rw and Rs showed different SD patterns for the two start locations (see Figure 7B), and knowing that start location has a strong effect on the grasp type, we zoomed in on the difference between the development of wrist and shoulder rotations, in relation to the grasp type (see Figure 8). The effect of cylinder height is stronger in the overlap-trials, as reflected in the steeper increasing SD patterns. This difference between grip strategy is strongest reflected in the shoulder rotation data.

4.1 Implications for Robotics

As stated in the Introduction, Obstacle avoidance is generally reflected in biphasic velocity profiles (Rosenbaum et al. 2001), The top panel of Figure 9 shows such a biphasic tangential grip velocity profile of a trial in which a 15-cm tall cylinder had to be grasped from S1. The lower panels show the whole trajectory of the lines connecting the centre of the handRB with the thumb and the index finger (like in Figure 3), and snapshots of the movement at 1, 20, 40, 50, 60, 70, 80, 90 and 100% of movement time. Although such biphasic tangential velocity profile is not recognisable in every trial, the idea of planning and executing movements with a bouncing posture, or through a via-point can be a valuable addition to the present anthropomorphic robot models [2]. A simulator can perform a similar task, and the tangential grip velocity is a variable that is easy to compare qualitatively. Figure 10 shows an example of a simulation of a trial (Start location 1, cylinder height = 15 cm) with obstacle avoidance characteristics. The panels show snapshots of a top view of the simulator at successive moments in time. The progress in time is indicated with a star shape on the biphasic tangential velocity profiles plotted in the left top of every panel.

In order to build anthropomorphic robots that have to interact with humans, it is convenient if these robots move like humans. Since humans are well trained in interpreting gestures and other movements of other humans, the intentions of a robot that behaves more humanlike, are recognised more easily and its human collaborator can smoothly adapt to this, which is safer, and facilitates the collaboration. But for safety reasons it is also a prerequisite that robots are able to avoid colliding into their human collaborators.

Our behavioural data show that the distal parts of the human prehension system are more flexible in adjusting to different target heights and starting positions or directions than the proximal parts. The snapshots of the ARoS robot simulator (Silva et al. in press) in Figure 10 also show the largest rotations in the distal joints while the simulator successfully approaches the cylinder while avoiding collisions with itself, the tabletop and the target. The present findings further illustrate that grasping an object from the side is not always the preferred

[2] It should be noted that not all trials showed such a biphasic pattern, and that the mean pattern of the tangential velocity shows a positively skewed bell shape. This can be explained by the relative difference in peak height between the first and second velocity peak and the fact that the second peak occurs at different moments across trials.

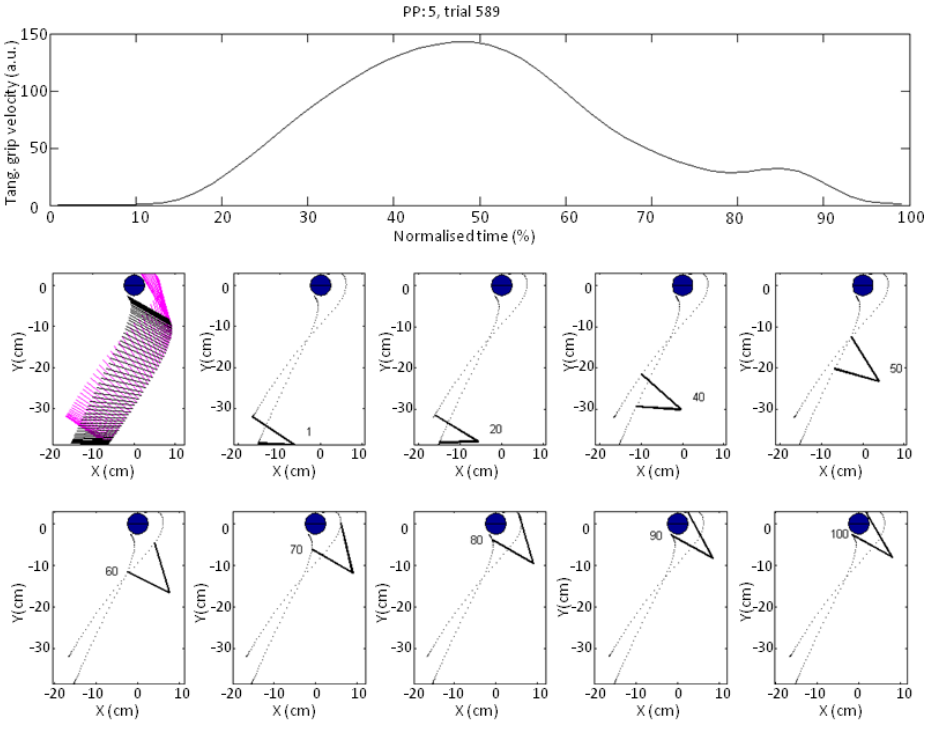

Fig. 9. Example of a trial (Start location 1, cylinder height = 15 cm) with obstacle avoidance characteristics. The top panel shows a biphasic tangential velocity profile and the other panels show estimates of the thumb and index finger movements in the horizontal plane at successive moments in time, the dashed lines show the trajectories of the thumb and index finger and the numbers indicate the relative moment during the response (in %).

option, therefore anthropomorphic robot models should have the flexibility to be able to approach and grasp target objects from above.

4.2 Alternative Approaches to Obstacle Avoidance in Robotics

The research on collision avoidance for movement of robotic manipulators can be divided into global and local methods. In global methods the collision avoidance is carried out by on-line algorithms before movement starts. On the other hand, in local methods, on-line algorithms are used in which possible collisions are tested during the motion, and the robot reacts by activating strategies to avoid obstacles when necessary.

Global methods include approaches where the motion planning is performed by searching for collision-free paths from start to goal configuration, in the robot's configuration space. Obstacles are mapped into this space as forbidden regions (for a review see Latombe 1999). Other methods treat the motion planning problem as an optimisation problem, where obstacles and joint limits are

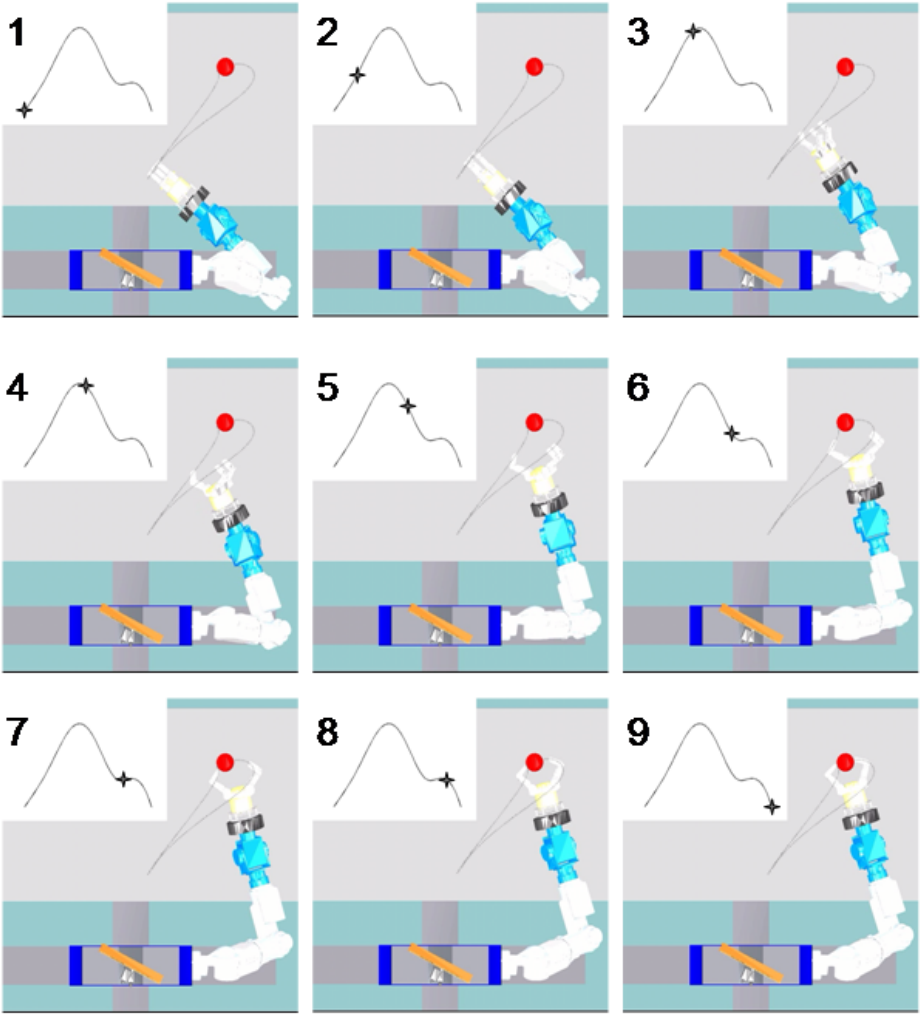

Fig. 10. Top view snapshots of the ARoS robot grasping a cylinder while avoiding collisions with itself, the tabletop and the target. Every panel shows the tangential velocity of the gripper in time, the star indicates the tangential velocity at the moment the snapshot was taken, the dashed lines show the trajectories of both sides of the gripper and the configuration of the robot's upper limb is shown at t=1, 20, 40, 50, 60, 70, 80, 90 and 100% of movement time in the successive panels from top left to bottom right.

the problem's constraints, and techniques like optimal control theory (Galicki 1998), nonlinear programming (Park 2006) and dynamic programming (Fiorini and Shiller 1996) are used.

Potential field methods are quite popular on-line collision avoidance methods for robot manipulators. These methods were first introduced by Khatib (1986),

and there is a large variety of these methods. At each step, the robot moves by following the gradient of a potential field consisting of attractive potentials, due to goal positions, repulsive potential due to obstacles and also repulsive potentials due to joint limits. Another local method is the attractor dynamics approach initially introduced for mobile robots (see e.g. Bicho 2000) and more recently to anthropomorphic robotic arms (Iossifidis and Schoner 2006). Here the time courses of the heading direction of the end effector, elevation and azimuth angles, and elbow motion were obtained from an attractor dynamics, into which obstacles contributed repulsive force-lets and joint limit constraints were coupled as repulsive force-lets as well.

In general alternative methods cannot produce human-like movements. However, experimental studies on human behaviour show that human-like movement facilitate interactions between robot and human. The movements of the anthropomorphic robot we have described before, are qualitatively similar to human movements, as is evident from our experimental and simulation results.

4.3 General Conclusion

We have found that humans avoid collisions while reaching to, and grasping cylinders by adjusting the movements of their distal joints. We successfully mimicked the resulting biphasic velocity profile in the ARoS simulation of a prehension and grasping movement like one of the conditions of our behavioural experiment. This validates the human-like movement characteristics of ARoS and, consequently, facilitates human-robot interaction.

Acknowledgements. This study was supported by the EU-funded project Joint-Action Science and Technology (JAST) (ref. IST-FP6-003747) and by FCT and UM through project "Anthropomorphic robotic systems: control based on the processing principles of the human and other primates motor system and potential applications in service robotics and biomedical engineering" (ref. CONC-REEQ/17/2001). Eliana Costa e Silva was supported by the Portuguese Foundation for Science and Technology (grant: FRH/BD/23821/2005). We would further like to acknowledge Wolfram Erlhagen and Estela Bicho (both at DEI, University of Minho, Portugal), Martin Butz and two anonymous reviewers for their comments on this paper.

References

1. Butz, M.V., Herbort, O., Hoffmann, J.: Exploiting redundancy for flexible behavior: unsupervised learning in a modular sensorimotor control architecture. Psychological Review 114(4), 1015–1046 (2007)
2. Bicho, E.: Dynamic Approach to Behavior-Based Robotics. Shaker-Verlag (2000)
3. Bouwhuisen, C.F., Meulenbroek, R.G.J., Thomassen, A.J.W.M.: A 3D motion-tracking method in graphonomic research: possible applications in future handwriting recognition studies. Pattern Recognition 35, 1039–1047 (2002)
4. Craig, J.J.: Introduction to robotics: mechanics and control. Addison-Wesley, Reading (1998)

5. Cuijpers, R.H., Smeets, J.B.J., Brenner, E.: On the relation between object shape and grasping kinematics. Journal of Neurophysiology 91(6), 2598–2606 (2004)
6. Edelman, S., Flash, T.: A model of handwriting. Biological Cybernetics 57(1-2), 25–36 (1987)
7. Elsinger, C.L., Rosenbaum, D.A.: End Posture selection in manual positioning: Evidence for feedforward modelling based on a movement choice methos. Experimental Brain Research 152, 499–509 (2003)
8. Erlhagen, W., Mukovskiy, A., Bicho, E., Panin, G., Kiss, C., Knoll, A., Van Schie, H.T., Bekkering, H.: Goal-directed imitation for robots: A bio-inspired appraoch to action understanding and skill learning. Robotics and autonomous systems 54(4), 353–360 (2006)
9. Fiorini, P., Shiller, Z.: Time Optimal Trajectory Planning in Dynamic Environments. In: Proc. of the IEEE Int. Conf. on Robotics and Automation, pp. 1553–1558 (1996)
10. Fischer, M.H., Rosenbaum, D.A., Vaughan, J.: Speed and sequential effects in reaching. Journal of Experimental Psychology-Human Perception and Performance 23(2), 404–428 (1997)
11. Galicki, M.: Robotics and Automation. In: Proc. of the IEEE Int. Conf. on Robotics and Automation, vol. 1, pp. 101–106 (1998)
12. Gréa, H., Desmurget, M., Prablanc, C.: Postural invariance in three-dimensional reaching and grasping movements. Experimental Brain Research 134, 155–162 (2000)
13. Iossifidis, I., Schöner, G.J.: Dynamical Systems Approach for the Autonomous Avoidance of Obstacles and Joint-limits for an Redundant Robot Arm. In: Proc. of the IEEE Int. Conf. on Intelligent Robots and Systems, pp. 508–585 (2006)
14. Jeannerod, M. (ed.): Intersegmental coordination during reaching at natural visual objects. Attention and Performace. Erlbaum, Hillsdale (1981)
15. Jeannerod, M.: The Timing of Natural Prehension Movements. Journal of Motor Behavior 16, 235–254 (1984)
16. Khatib, O.: Real-Time Obstacle Avoidance for Manipulators and Mobile Robots. The International Journal of Robotics Research 5(1), 90–98 (1986)
17. Klein Breteler, M.D., Meulenbroek, R.G.J.: Modeling 3D object manipulation: synchronous single-axis joint rotations? Experimental Brain Research 168(3), 395–409 (2006)
18. Kritikos, A., Bennett, K.M.B., Dunai, J., Castiello, U.: Interference from distractors in reach-to-grasp movements. Quarterly Journal of Experimental Psychology Section a-Human Experimental Psychology 53(1), 131–151 (2000)
19. Latombe, J.: Motion Planning: A journey of robots. molecules, digital actors, and other artifacts. International Journal of Robotics Research, 1119–1128 (1999)
20. Meegan, D.V., Tipper, S.P.: Reaching into cluttered visual environments: spatial and temporal influences of distracting objects. Quarterly Journal of Experimental Psychology 51(2), 225–249 (1998)
21. Meulenbroek, R.G.J., Rosenbaum, D.A., Jansen, C., Vaughan, J., Vogt, S.: Multijoint grasping movements - Simulated and observed effects of object location, object size, and initial aperture. Experimental Brain Research 138(2), 219–234 (2001)
22. Osheron, D.N., Kosslyn, S.M., Hollerbach, J.M. (eds.): Visual Cognition in Action: an Invitation to Cognitive Science. MIT Press, Cambridge (1990)
23. Park, J.: Optimal Motion Planning for Manipulator Arms Using Nonlinear Programming. In: Huat, L.K. (ed.) Industrial Robotics, Programming, Simulation and Applications, pp. 256–272. pIV pro literatur Verlag Robert Mayer-Scholz (2006)

24. Paulignan, Y., Frak, V.G., Toni, I., Jeannerod, M.: Influence of object position and size on human prehension movements. Experimental Brain Research 114, 226–234 (1997)
25. Rosenbaum, D.A.: Human Motor Control. Academic Press, San Diego (1990)
26. Rosenbaum, D.A., Meulenbroek, R.G.J., Vaughan, J.: Planning Reaching and Grasping Movements: Theroretical Premises and Practical Implications. Motor Control. 2, 99–115 (2001)
27. Rosenbaum, D.A., Meulenbroek, R.G.J., Vaughan, J.: Coordination of reaching and grasping by capitalizing on obstacle avoidance and other constraints. Experimental Brain Research 128(1-2), 92–100 (1999)
28. Rosenbaum, D.A., Meulenbroek, R.G.J., Vaughan, J., Jansen, C.: Posture-based motion planning: Applications to grasping. Psychological Review 108(4), 709–734 (2001)
29. Silva, R., Bicho, E., Erlhagen, W.: AROS: An anthropomorphic robot for human-robot interaction and coordination studies. In: Proc. of the Portuguese 8th Conference on Automatic Control - Controlo 2008, pp. 819–826 (2008)
30. Smeets, J.B.J., Brenner, E.: A New View on Grasping. Motor Control 3, 237–271 (1999)
31. Smeets, J.B.J., Brenner, E.: Independent movements of the digits in grasping. Experimental Brain Research 139, 92–100 (2001)
32. Soechting, J.F., Buneo, C.A., Herrmann, U., Flanders, M.: Moving Effortlessly in 3-Dimensions: Does Donders-Law Apply to Arm Movement. Journal of Neuroscience 15(9), 6271–6280 (1995)
33. Vaughan, J., Rosenbaum, D.A., Meulenbroek, R.G.J.: Planning Reaching and Grasping Movements: The Problem of Obstacle Avoidance. Motor Control 2, 116–135 (2001)
34. Vaughan, J., Rosenbaum, D.A., Meulenbroek, R.G.J.: Modeling Reching and Manipulating in 2- and 3-D Workspaces: The Posture-Based Model. ICDL, Bloomington (2006)